

# Crystalline Regions of *Bombyx mori* Silk Fibroin May Exhibit $\beta$ -Turn and $\beta$ -Helix Conformations

N. D. Lazo and Donald T. Downing\*

Marshall Dermatology Research Laboratories, Department of Dermatology, University of Iowa College of Medicine, Iowa City, Iowa 52242

Received January 15, 1999; Revised Manuscript Received May 6, 1999

**ABSTRACT:** Modeling of the (GSGAGA)<sub>n</sub> consensus sequence of the crystalline region of *Bombyx mori* silk fibroin revealed two novel conformations. One was a series of four-residue  $\beta$ -turns, consistent with published circular dichroic spectra and nuclear magnetic resonance data for the water-soluble silk I that is found in the abdominal glands of the silkworm larvae before spinning. The other conformation was a single-chain  $\beta$ -helix having 4.3 residues per turn, consistent with the circular dichroic spectra and water insolubility of silk II, the fibrous form of silk fibroin. Computer modeling of these structures provided a conformational energy of  $-9.9 \text{ kcal mol}^{-1} \text{ residue}^{-1}$  for an isolated strand of continuous  $\beta$ -turns,  $-11.7 \text{ kcal mol}^{-1} \text{ residue}^{-1}$  for a strand of  $\beta$ -turns on the edge of a sheet of parallel strands,  $-14.9 \text{ kcal mol}^{-1} \text{ residue}^{-1}$  for a strand of  $\beta$ -turns embedded in a parallel array of  $\beta$ -turns, and  $-13.0 \text{ kcal mol}^{-1} \text{ residue}^{-1}$  for an isolated, right-handed  $\beta$ -helix. These values are consistent with the transformation of silk I to silk II when an aqueous solution of silk fibroin is subjected to shear. The synthetic consensus peptide Ac-(GSGAGA)<sub>2</sub>NH<sub>2</sub> had a circular dichroic spectrum characteristic of the  $\beta$ -helical conformation and formed long, curving fibrils that were measured on electron micrographs as having a 2 nm diameter.

## 1. Introduction

Larvae of the silk moth *Bombyx mori* weave their cocoons from a concentrated protein solution that is stored in abdominal glands. During spinning, the shearing forces inherent in extrusion change the conformation of the soluble silk fibroin, designated silk I, into the fibrous form, silk II. Despite extensive investigation, the molecular conformation of silk I has remained unclear,<sup>1–10</sup> while the structure proposed for silk II, long regarded as a prime example of the  $\beta$ -sheet conformation,<sup>1,2,5–11</sup> continues to be investigated.<sup>12</sup>

In the  $\beta$ -sheet conformation as applied to silk II, extended polypeptide chains are thought to run parallel to the fiber axis, while the hydrogen bonds between peptide carbonyl oxygens and amide protons of adjacent  $\beta$ -strands are perpendicular to the fiber axis.<sup>11,12</sup> In the radial direction that is perpendicular to the  $\beta$ -strands, the  $\beta$ -sheets are stacked, with attraction within pairs of sheets being attributed to hydrophobic interactions.<sup>9,10</sup> However, the alanine and serine residues that alternate with glycines in the consensus sequence (GSGAGA)<sub>n</sub> are not sufficiently bulky or hydrophobic to provide a strong cohesive force within pairs of  $\beta$ -sheets. Second, the pairs of sheets that are viewed as held together by hydrophobic interactions have only glycines apposed in the alternating intersheet regions, with no ionic, hydrophobic, or hydrogen-bonding interactions to provide cohesion. Third, assuming there is a means of maintaining cohesion between all of the stacked sheets, it is unclear what factor causes termination in the stacking direction to provide a fibrillar structure rather than a laminar sheet of indeterminate breadth.

Recently, we proposed that certain fibrous proteins may contain a new protein conformation that has been termed the  $\beta$ -helix.<sup>13</sup> Several examples of such  $\beta$ -helical

structures have been established by X-ray crystallography of the pectate lyases,<sup>14</sup> phage tailspikes,<sup>15,16</sup> viral fibers,<sup>17</sup> and an acyltransferase.<sup>18</sup> Longer courses of uninterrupted  $\beta$ -helix have been proposed for specific domains in intermediate-filament proteins<sup>19–21</sup> and their synthetic peptide analogues.<sup>22,23</sup> In the present study, we examined the possibility that the physical properties of *B. mori* silk might be better explained as containing regions of  $\beta$ -helix. By molecular modeling of silk primary sequences, we discovered a plausible new form of the  $\beta$ -helical conformation in which all amino acid side chains are arrayed on the exterior of a single-chain  $\beta$ -helix, allowing much tighter helices than previously envisioned. A synthetic peptide (GSGAGA)<sub>2</sub>, representing the consensus sequence of the crystalline regions of silk fibroin, provided supporting spectra and formed 2 nm diameter fibers characteristic of  $\beta$ -helical aggregates.

In addition, we interpret published circular dichroic (CD) spectra to indicate that silk I consists almost exclusively of a continuous series of four-residue  $\beta$ -turns, a metastable aggregation of which is poised for transformation into the  $\beta$ -helices of silk II during the spinning of fibers by the silkworm. Computer modeling of each of the conformations postulated for silk fibroin revealed conformational energies consistent with stable, unstrained structures.

## 2. Experimental Section

**Computer Modeling.** CPK models of the conformations applied to the analogue (GSGAGA)<sub>6</sub> are shown in Figure 1. Molecular modeling of the conformations was performed on a Silicon Graphics Indigo workstation, using SYBYL 6.4 software. For modeling a continuous series of  $\beta$ -turns for silk I, the serines and alanines were assigned backbone dihedral angles ( $\phi$ ,  $\psi$ ) of  $-60^\circ$  and  $120^\circ$ , respectively, while the glycines were assigned ( $\phi$ ,  $\psi$ ) angles of  $80^\circ$  and  $0^\circ$ , respectively. In addition, a hydrogen bond was specified, for each turn, between the carbonyl oxygen of the first glycine and the amino proton of the fourth residue (alanine or serine). The conformational

\* To whom correspondence should be addressed. Phone: (319) 335-8077. Fax: (319) 335-9559. E-mail: noel-lazo@uiowa.edu.

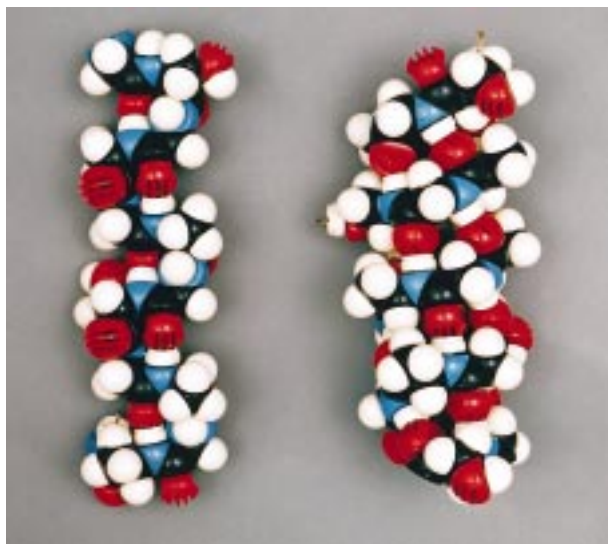


**Figure 1.** CPK models of the consensus sequence (GSGAGA)<sub>n</sub> in the  $\beta$ -turn conformation postulated for silk I (left) and the  $\beta$ -helix postulated for silk II (right).

energy of the structure was minimized, using the Kollmann all-atom force field and Kollmann charges, until convergence.

To form a sheet of  $\beta$ -turn strands, copies of the 36-residue  $\beta$ -turn strand conformation were arrayed in parallel, with the serine residues in register, and intermolecular hydrogen bonds were specified between the carbonyl oxygens of the even-numbered residues in each strand and the amino protons of the closest glycines in adjacent strands. A dimer and a trimer were each subjected to energy minimization. The conformational energy of one  $\beta$ -turn strand in the dimer was taken to represent the energy of strands along the edges of any sheet containing two or more strands. Subtraction of the energy of the dimer from the energy of the trimer was assumed to provide the energy of individual strands embedded in sheets containing three or more strands. Similar energies were obtained when the structures were first subjected to annealing, with shake enabled, followed by energy minimization.

For modeling the single-chain  $\beta$ -helix, the sequence (GS-GAGA)<sub>6</sub> was first assigned the extended  $\beta$ -strand conformation. Then, hydrogen bonds were specified as constraints in folding the molecule into helices. For a left-handed  $\beta$ -helix, each glycine (*i*) carbonyl oxygen was bonded to the amino proton of the residue in the *i* + 5 position; in addition, each glycine amino proton was hydrogen-bonded to the carbonyl oxygen of the residue in the *i* + 3 location. For a right-handed  $\beta$ -helix, each glycine carbonyl oxygen was hydrogen-bonded to the amino proton of the residue in the *i* - 3 position, and the glycine amino protons were hydrogen-bonded to the carbonyl oxygens of residues in the *i* - 5 positions. Each hydrogen bond was converted to two distance constraints:  $d_{\text{NO}} = 2.9\text{--}3.2$  Å and  $d_{\text{OH}} = 1.9\text{--}2.2$  Å. The structures were annealed with shake enabled, during which the  $\beta$ -helical conformation was adopted, and then energy minimization was carried out to convergence.

Arrays of  $\beta$ -strands and  $\beta$ -turn strands were also modeled in which several of the planar sheets were stacked in the third dimension and then energy-minimized. The energy of a stack made up of two sheets was taken to represent the energy of sheets at the top and bottom of a stack. The energy of an internal sheet in a stack was obtained by subtracting the energy of a two-sheet stack from that of a three-sheet stack. A similar procedure was used for obtaining the energy of  $\beta$ -helices packed in layers.

**Peptide Synthesis.** The peptide Ac(GSGAGA)<sub>2</sub>NH<sub>2</sub>, representing the consensus sequence of the crystalline regions of *B. mori* silk, was synthesized manually using standard solid-phase synthesis, as described previously.<sup>22,23</sup> The peptide was purified to >95% by reversed-phase HPLC, and its identity was verified by electrospray mass spectrometry. The peptide

was sparingly soluble in water but was soluble in dimethyl sulfoxide (DMSO).

**Circular Dichroism.** Cast films of the synthetic peptide were prepared by placing 10–30  $\mu$ L of its DMSO solution on the quartz windows of demountable CD cells and allowing them to dry in a desiccator over Drierite. Conventional UV spectra were obtained on the cast films, using a Beckman DU 1500 spectrophotometer. The same cast films were then placed in a CD spectrometer (Aviv Associates model 62DS), and the far-UV spectra to 190 nm were obtained, using an averaging time of 12 s. The mean-residue ellipticity spectrum was calculated using the formula

$$[\theta] = \frac{[\theta]_{\text{obs}}}{10cl}$$

where  $[\theta]$  is the mean-residue ellipticity in units of deg cm<sup>2</sup> dmol<sup>-1</sup>,  $[\theta]_{\text{obs}}$  is the observed ellipticity in millidegrees, *c* is the concentration in moles (equivalents) of peptide bond per liter, and *l* is the path length in centimeters. The combined value for *cl* was obtained from the measured UV spectrum, using the relationship

$$cl = A_{192}/\epsilon_{192}$$

where  $A_{192}$  is the measured absorbance of the cast peptide film at 192 nm,  $\epsilon_{192}$  is a published value (10 000) for the molar extinction coefficient for the peptide carbonyl at 192 nm,<sup>25</sup> *c* is the concentration of peptide bond in molar equivalents per liter, and *l* is the path length in centimeters.

**Electron Microscopy.** A solution of the synthetic peptide in DMSO that was frozen at -20 °C and then thawed was found to contain a suspension of finely dispersed solids. A drop of the suspension was placed on a Formvar coated copper grid, excess solvent was wicked off, and the remaining deposit was stained with uranyl acetate. Specimens were also prepared by evaporating a drop of the DMSO solution on a grid at room temperature and then staining with uranyl acetate. The preparations were examined in an electron microscope (Hitachi model H7000) at 30000 $\times$  magnification, and the negative images were magnified a further 3 $\times$  in photographic prints. Many fields contained very long fibrils having a uniform diameter, which was measured using a graduated loupe.

### 3. Results and Discussion

**Silk I.** CD spectra of silk I published by previous investigators<sup>1,2,7</sup> have shown a single excursion at 199 nm having a  $[\theta]$  value of about -5000 deg cm<sup>2</sup> dmol<sup>-1</sup>, which they interpreted as a weak random coil signal. However, the negligible ellipticity ( $[\theta] \approx 0$ ) above 210 nm shows the absence of both  $\alpha$ -helix and  $\beta$ -sheet conformations, while an exclusively random coil conformation should have  $[\theta]_{200} \approx -40\,000$  deg cm<sup>2</sup> dmol<sup>-1</sup>.<sup>23</sup> Therefore, we conclude that the conformation of silk I is predominantly  $\beta$ -turn, which has been calculated to have a single weak negative CD signal near 200 nm that is one-fifth to one-tenth as strong as that of a random coil.<sup>26</sup> Computer modeling of an isolated  $\beta$ -turn conformation proposed for Ac(GSGAGA)<sub>6</sub>NH<sub>2</sub> yielded a conformational energy of -9.9 kcal mol<sup>-1</sup> residue<sup>-1</sup> (Table 1), indicating a stable conformation. Each residue in a two-strand parallel array of  $\beta$ -turn strands had an energy of -11.7 kcal/mol, while the central strand in a three-molecule parallel array (Figure 2), with maximal intermolecular hydrogen bonding, had an energy of -14.9 kcal mol<sup>-1</sup> residue<sup>-1</sup>. Table 2 contains the conformational energies of three-dimensional arrays of  $\beta$ -strands and  $\beta$ -turn strands that were computed using stacks of two or three of the sheets of strands described above.

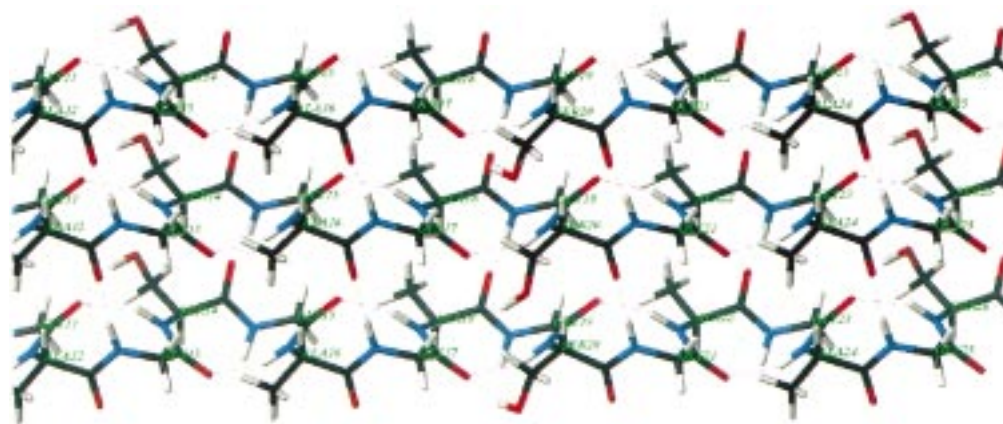


**Figure 2.** Part of the energy-minimized model of the consensus sequence (GSGAGA)<sub>6</sub> in the continuous  $\beta$ -turn conformation postulated for silk I, shown as a three-chain parallel array. Broken lines indicate hydrogen bonds.

**Table 1. Calculated Energies for Proposed Conformations of (GSGAGA)<sub>6</sub>**

conformation	minimum energy (kcal mol <sup>-1</sup> residue <sup>-1</sup> )
$\beta$ -strand	
isolated	-6.7
edge of antiparallel $\beta$ -sheet	-10.0
interior of antiparallel $\beta$ -sheet	-12.5
$\beta$ -turn strand	
isolated	-9.9
edge of $\beta$ -turn sheet	-11.7
interior of $\beta$ -turn sheet	-14.9
$\beta$ -helix	
right-handed	-13.0
left-handed	-11.4

**Table 2. Calculated Energies for Proposed Conformations of Three Sheets of (GSGAGA)<sub>6</sub>**

conformation	minimum energy (kcal mol <sup>-1</sup> residue <sup>-1</sup> )
<b>Silk I</b>	
$\beta$ -turn sheets	
isolated	-12.8
edge sheets	-13.6
interior sheet	-14.3
<b>Silk II</b>	
$\beta$ -sheets	
isolated	-10.7
edge sheets	-12.0
interior sheet	-13.2
$\beta$ -helices	
isolated layer of three helices	-13.5
outer layers of two layers of three helices each	-13.9
interior layer of three layers of three helices each	-14.1

The computed backbone torsion angles (Table 3) for the Ala and Ser residues in silk I fell within regions of contour plots  $\Delta(\phi, \psi)$  that satisfy the conformation-dependent <sup>13</sup>C NMR chemical shifts of both the C<sub>α</sub> and C<sub>β</sub> carbons of the two residues.<sup>27</sup> However, the pattern of torsion angles of successive residues in the energy-minimized structure matched none of the pairs of dihedral angles that have been reported for the two central residues in recognized types of  $\beta$ -turn.<sup>28–30</sup> The  $\phi, \psi$  angles computed for serine and alanine residues in  $i + 1$  positions in the continuous  $\beta$ -strands matched those reported for type II  $\beta$ -turns, while the angles for the glycine residues in  $i + 2$  positions matched those of type III'  $\beta$ -turns. Thus, the unique conditions imposed by the continuous  $\beta$ -turn conformation appear to generate a new type of  $\beta$ -turn.

**Table 3. Torsion Angles Calculated for Computed Silk Conformations**

residue	silk I ( $\beta$ -turns)		silk II ( $\beta$ -helix)	
	$\phi$ (deg)	$\psi$ (deg)	$\phi$ (deg)	$\psi$ (deg)
Gly 1	64	29	142	-83
Ser 2	-56	118	-76	86
Gly 3	59	30	138	-83
Ala 4	-59	119	-73	82
Gly 5	65	28	139	-83
Ala 6	-57	115	-73	85
Gly 7	64	32	137	-84
Ser 8	-59	122	-73	84
Gly 9	60	29	137	-83
Ala 10	-58	117	-73	83
Gly 11	63	29	139	-83
Ala 12	-57	120	-73	85

The continuous  $\beta$ -turn structure that we propose for silk I has similarities to an earlier "crankshaft" conformation that was suggested for the poly(L-Ala-Gly) analogue of silk fibroin, based on electron and X-ray diffraction data.<sup>3,10</sup> The chain axis repeat distance of four residues was reported as 9.6 Å for the crankshaft model polypeptide, the same distance we measured on a space-filling model of the silk I  $\beta$ -turn conformation (Figure 1). The lateral packing distance of the crankshaft polypeptide chains was estimated from the unit cell dimensions as 7.2 Å,<sup>3,10</sup> which coincides with the corresponding measurement made on the space-filling CPK model of a two-dimensional array of  $\beta$ -turns. A major difference between the two conformations is that in the "crankshaft" model, the peptide carbonyl groups were oriented in pairs perpendicular to the axis,<sup>10</sup> while in our model the carbonyl orientations alternate between axial (hydrogen-bonded intramolecularly) and radial (hydrogen-bonded intermolecularly in arrays), with successive radially oriented carbonyls alternating in direction toward opposite sides of the strand (Figure 2). It seems probable that these relative carbonyl orientations are responsible for the extremely weak CD ellipticity of the  $\beta$ -turn structure. It may also be observed that the amino acid side chains of our  $\beta$ -turn strand alternate in direction between one side and the other.

Computer modeling in the present study clearly indicated that a  $\beta$ -turn strand, in which intermolecular hydrogen bonding was maximized in a two-dimensional sheet array, had the lowest energy (Table 1) and was therefore the most stable conformation. Furthermore, our energy minimization results also show that an





**Figure 3.** Electron micrograph of fibrils formed by the synthetic peptide  $\text{Ac}(\text{GSGAGA})_2\text{NH}_2$ , an analogue of silk II, crystallized from DMSO. Similar fibrils were obtained by evaporation of the DMSO solution on a Formvar coated grid. Bar = 100 nm.

isolated  $\beta$ -turn strand is more stable than an isolated conventional  $\beta$ -strand (Table 1). These results are in line with our proposition that the concentrated solution of silk I, which is secreted in the silk glands of *B. mori* and which is stable for long periods, has the  $\beta$ -turn sheet conformation. This may explain why in vivo biosynthesis of silk fibroin yields a solution of  $\beta$ -turn strands rather than  $\beta$ -sheets. The idea that the proposed  $\beta$ -turn strand conformation is the more stable is also in line with the knowledge that after dissolving silk II in lithium bromide, dialysis against water results in restoration of the silk I conformation.<sup>1,5,8</sup> It is possible to propose an array of  $\beta$ -turn sheets that are stacked in the third dimension (Table 3). However, there may be little impetus for additional ordering, limited to hydrogen bonding between serine side chains, and the questionable hydrophobic interactions between sheets of alanine side chains. Furthermore, three-dimensional association would inevitably lead to macroscopic aggregation and precipitation, which do not occur even in the highly concentrated solutions of silk I in the abdominal glands (or in vitro) until shear forces precipitate the transformation to silk II.

**Silk II.** The consensus peptide  $\text{Ac}(\text{GSGAGA})_2\text{NH}_2$  that we synthesized as a model for silk fibroin was found to crystallize in long fibrils from DMSO (Figure 3). When a DMSO solution of the peptide was allowed to dry on a quartz plate, the CD spectrum (Figure 4) was similar to that calculated for a 100%  $\beta$ -helix<sup>31</sup> and to that measured for a previously synthesized  $\beta$ -helical peptide.<sup>22</sup> However, the CD spectrum for the present synthetic peptide was more intense at 198 nm, while the minimum was weaker and occurred at 221 nm rather than at 217 nm as reported for previous  $\beta$ -helices.<sup>13,22,23</sup> For the consensus sequence  $(\text{GSGAGA})_n$  it was

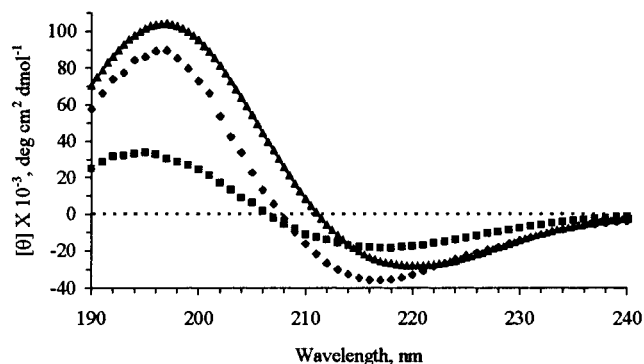


**Figure 4.** CD spectrum of a film of synthetic peptide  $\text{Ac}(\text{GSGAGA})_2\text{NH}_2$  cast from solution in DMSO (triangles), compared with the spectra of a 100%  $\beta$ -helix calculated for pectate lyases<sup>31</sup> (diamonds) and poly(L-lysine) (squares), a commonly used standard for  $\beta$ -sheet conformation.<sup>25</sup>

possible to construct a helix in which serine and alanine were tightly packed in the helix lumen, as for the bulkier hydrophobic groups in previously reported  $\beta$ -helices.<sup>13,22,23</sup> However, this construction seemed unlikely to be stable because the external glycine residues would provide no protection from the attack of solvent water on the peptide backbone hydrogen bonding. Also, alanine is recognized as being quite ambivalent regarding hydrophilic/hydrophobic effects and, in concert with serine, would be unlikely to provide much hydrophobic impetus in folding the molecule. Furthermore, there seemed to be no way to incorporate the occasional bulkier hydrophobic groups (valine and tyrosine) into the helix lumen. Therefore, we examined the possibility that the silk II structure consists of an everted helix, in which the serine and alanine residues are arrayed on the exterior of the helix, as shown in Figure 1.

Computer-generated models (Figure 5) revealed that single-chain  $\beta$ -helices could be constructed in which the central lumen (1.7 Å diameter from the CPK model in Figure 1) was small enough to completely exclude water, while the serine and alanine residues occupied the external surface. Exclusion of water from the helix lumen would seem to be important in reducing the attack of water on the hydrogen bonding between peptide carbonyl oxygens and amide protons in successive turns of the helix. In the single-chain parallel helix, because of its tight curvature, the backbone hydrogen bonds appeared to be much less strained than is the case in planar parallel  $\beta$ -sheets. Half of the hydrogen bonds, in which the glycine carbonyls were directed toward the carboxyl terminal, were almost parallel with the axis of the helix, and the  $\text{C}=\text{O}\cdots\text{H}-\text{N}$  alignment was close to 180°. The remaining hydrogen bonds in the single-chain helix were distinctly nonlinear and formed an angle of about 20° with the helix axis. In the energy-minimized computer model of the right-handed single-chain helix (Figure 5) the computed free energy was  $-13.0 \text{ kcal mol}^{-1} \text{ residue}^{-1}$ , distinctly more stable than the  $-11.4 \text{ kcal mol}^{-1} \text{ residue}^{-1}$  for the left-handed conformation (Table 1). The isolated right-handed  $\beta$ -helix was much more stable than either the isolated  $\beta$ -turn strand ( $-9.9 \text{ kcal mol}^{-1} \text{ residue}^{-1}$ ) or even a  $\beta$ -turn strand hydrogen-bonded on one side to the edge of a parallel array ( $-11.7 \text{ kcal mol}^{-1} \text{ residue}^{-1}$ ). However, a  $\beta$ -turn strand fully embedded in a parallel array and hydrogen-bonded to like molecules on both sides had by far the lowest energy ( $-14.9 \text{ kcal mol}^{-1} \text{ residue}^{-1}$ ) of all the conformers evaluated.

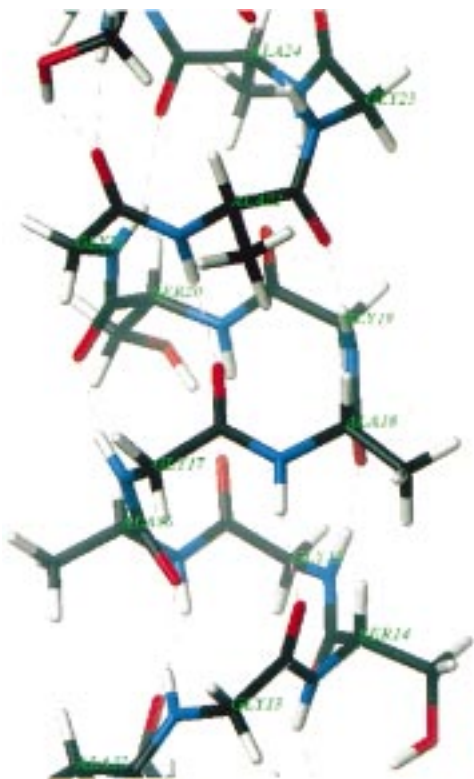


**Figure 5.** Computer model of the consensus sequence (GS-GAGA)<sub>6</sub> in the right-handed  $\beta$ -helix postulated for silk II.

Table 2 shows calculated energies for proposed conformations of silk II formed from three sheets of (GS-GAGA)<sub>6</sub>. An isolated layer of three  $\beta$ -helices has a lower energy than any of the three types of  $\beta$ -sheets considered in Table 2. With packing of the  $\beta$ -helices, the calculated energies became lower but not as low as that for an interior  $\beta$ -turn sheet (Tables 1 and 2).

Published CD spectra for silk II consistently show a single negative excursion near 220 nm with  $[\theta] \approx -10\,000 \text{ deg cm}^2 \text{ dmol}^{-1}$  and a positive peak near 200 nm,  $[\theta] \approx 20\,000\text{--}30\,000 \text{ deg cm}^2 \text{ dmol}^{-1}$ . This spectral shape is roughly consistent with the  $\beta$ -conformation but is only about  $1/4$  of the intensity expected for a 100%  $\beta$ -helix.<sup>22,31</sup> If substantial amounts of random coil were present, the signal at 200 nm would be weak or negative. However, if  $\beta$ -turn were present, the weak CD intensity of the  $\beta$ -turn could dilute the  $\beta$ -helix signal without introducing substantial CD ellipticities of its own. It may be significant that the negative CD ellipticity reported for silk II is at almost the same wavelength as that of our synthetic consensus peptide.

X-ray diffraction studies<sup>6,7,10,11</sup> of silk fiber have provided atomic spacing data that have been interpreted in terms of a  $\beta$ -sheet conformation. However, interchain spacing and in-strand distances are similar for  $\beta$ -sheet and  $\beta$ -helix and are therefore not definitive. Also, stacking distances between  $\beta$ -sheets may be mimicked by intermolecular distances between stacked  $\beta$ -helices. An X-ray periodicity of 21 Å from silk II has been attributed to the serine repeats in linear  $\beta$ -strands of the consensus sequence; remarkably, the same distance between serines is found in CPK models of our consensus peptide whether modeled as  $\beta$ -sheet or as  $\beta$ -helix. In summary, X-ray diffraction data may support the  $\beta$ -helix conformation as well as the conventional  $\beta$ -sheet conformation.

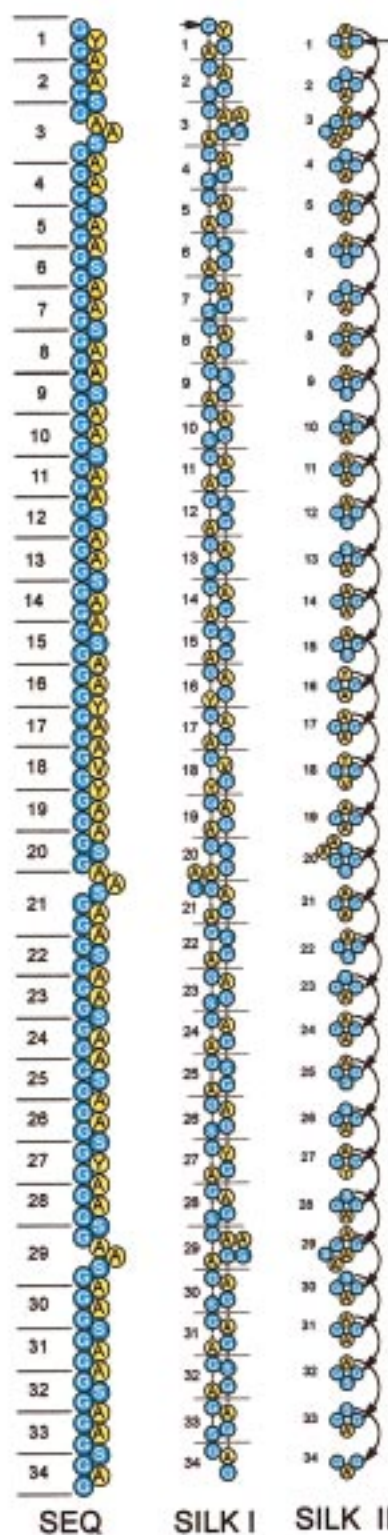


**Figure 6.** Drawings of the primary sequence and the  $\beta$ -turn and  $\beta$ -helix conformations for a crystalline region of *B. mori* silk fibroin. The sequence is arranged to emphasize the alternation of glycine residues and the preservation of alternation with lateral loops. Numbers indicate the same successive groups in each conformation, and arrows indicate the transitions between successive turns of the  $\beta$ -helix.

**Conformational Transitions of Silk Fibroin.** Our results from computer modeling suggest that when a monolithic array of  $\beta$ -turn conformation is disrupted, as by shear, the strands at the newly generated edges will have an impetus to adopt the  $\beta$ -helical conforma-

tion. This would expose another  $\beta$ -turn strand ready to assume the  $\beta$ -helical structure, and so on, providing an explanation for the rapid transformation of silk I to silk II by the shearing forces inherent in spinning or stirring.

Conversion of silk I to silk II may require only a simple collapse of the series of four-residue  $\beta$ -turns to form the single-chain  $\beta$ -helix, also having approximately four residues per turn, that we propose for silk II. Drawings of the primary sequence and the  $\beta$ -turn and  $\beta$ -helix conformations for the crystalline regions of *B. mori* silk fibroin are shown in Figure 6. The conformational energy that we computed for the  $\beta$ -turn conformation of silk I embedded in the two-dimensional array ( $-14.9 \text{ kcal mol}^{-1} \text{ residue}^{-1}$ ) is much lower than the energy of the isolated  $\beta$ -turn conformation ( $-9.9 \text{ kcal mol}^{-1} \text{ residue}^{-1}$ ), or even a  $\beta$ -turn strand at the edge of an array of like molecules ( $-11.7 \text{ kcal mol}^{-1} \text{ residue}^{-1}$ ). Therefore, considerable energy must be supplied in order to disrupt the liquid-crystalline array that we postulate for silk I. However, once an individual  $\beta$ -turn strand is exposed, its conformation may be transformed into the  $\beta$ -helical conformation, which is more stable as an isolated strand. This may explain why shearing forces result in rapid transformation of silk I into silk II.

#### 4. Conclusions

To date, a few  $\beta$ -helical protein structures have been firmly established by X-ray crystallography<sup>14–18</sup> and additional examples have been proposed from analysis of sequences, physical properties, and electron microscopic evidence.<sup>13,19–23</sup> The present study proposes a variation of the  $\beta$ -helical conformation and demonstrates by energy-minimization computations that the structures that we propose for silk II should be favored energetically over the  $\beta$ -sheet conformation currently accepted. Energy calculations also support the  $\beta$ -turn conformation that we propose for silk I, which is consistent with the circular dichroism spectra and nuclear magnetic resonance data obtained by previous investigators.

**Acknowledgment.** This work was supported in part by NIH Grant AR32374, by a Medical Research Initiative Grant from the Carver Trust, University of Iowa College of Medicine, and by a bequest from the Carl J. Hertzog Foundation. The peptide analogue was synthesized in the Protein Structure Facility, electron microscopy was carried out by the Central Microscope Facility,

peptide mass spectra were obtained by the Mass Spectrometry Facility, and computer modeling was conducted in the Image Analysis Facility, all facilities operated by the University of Iowa.

#### References and Notes

- (1) Iisuka, E.; Yang, J. T. *Proc. Natl. Acad. Sci. U.S.A.* **1966**, *55*, 1175.
- (2) Iisuka, E.; Yang, J. T. *Biochemistry* **1968**, *7*, 2218.
- (3) Lotz, B.; Keith, H. D. *J. Mol. Biol.* **1971**, *61*, 201.
- (4) Asakura, T.; Watanabe, Y.; Uchida, A.; Minagawa, H. *Macromolecules* **1984**, *17*, 1075.
- (5) Saitô, H.; Tabeta, R.; Asakura, T.; Iwanaga, Y.; Shoji, A.; Azaki, T.; Anda, Y. *Macromolecules* **1984**, *17*, 1405.
- (6) Asakura, T.; Kuzuhara, A.; Tabeta, R.; Saitô, H. *Macromolecules* **1985**, *18*, 1841.
- (7) Canetti, M.; Seves, A.; Secundo, F.; Vecchio, G. *Biopolymers* **1989**, *28*, 1613.
- (8) Ishida, M.; Asakura, T.; Yokoi, M.; Saitô, H. *Macromolecules* **1990**, *23*, 88.
- (9) Fossey, S. A.; Némethy, G.; Gibson, K. D.; Scheraga, H. A. *Biopolymers* **1991**, *31*, 1529.
- (10) Lotz, B.; Cesari, F. C. *Biochimie* **1979**, *61*, 205.
- (11) Marsh, R. E.; Corey, R. B.; Pauling, L. *Biochim. Biophys. Acta* **1955**, *16*, 1.
- (12) Nicholson, L. K.; Asakura, T.; Demura, M.; Cross, T. A. *Biopolymers* **1993**, *33*, 847.
- (13) Lazo, N. D.; Downing, D. T. *Biochemistry* **1998**, *37*, 1731.
- (14) Yoder, M. D.; Keen, N. T.; Jurnak, F. *Science* **1993**, *260*, 1503.
- (15) Steinbacher, S.; Seckler, R.; Miller, S.; Steipe, B.; Huber, R.; Reinemer, P. *Science* **1994**, *265*, 383.
- (16) Cerritelli, M. E.; Wall, J. S.; Simon, M. N.; Conway, J. F.; Steven, A. C. *J. Mol. Biol.* **1996**, *260*, 767.
- (17) Stouten, P. F. W.; Sander, C.; Ruigrk, R. W. H.; Cusack, S. *J. Mol. Biol.* **1992**, *226*, 1073.
- (18) Raetz, C. R. H.; Roderick, S. L. *Science* **1995**, *270*, 997.
- (19) Downing, D. T. *Proteins: Struct. Funct. Genet.* **1995**, *23*, 204.
- (20) Downing, D. T. *Proteins: Struct. Funct. Genet.* **1996**, *25*, 215.
- (21) Downing, D. T. *Proteins: Struct. Funct. Genet.* **1996**, *26*, 472.
- (22) Lazo, N. D.; Downing, D. T. *Biochem. Biophys. Res. Commun.* **1997**, *235*, 675.
- (23) Lazo, N. D.; Downing, D. T. *J. Pept. Res.* **1998**, *51*, 85.
- (24) Woods, A. H.; O'Bar, P. R. *Science* **1970**, *167*, 179.
- (25) Yang, J. T.; Wu, C.-S. C.; Martinez, H. M. *Methods Enzymol.* **1986**, *130*, 208.
- (26) Perczel, A.; Hollósi, M. In *Circular Dichroism and the Conformational Analysis of Biomolecules*; Fasman, G. D., Ed.; Plenum Press: New York, 1996; pp 285–381.
- (27) Asakura, T.; Demura, M.; Date, T.; Miyashita, N.; Ogawa, K.; Williamson, M. P. *Biopolymers* **1997**, *41*, 193.
- (28) Chou, P.; Fasman, G. D.  $\beta$ -Turns in Proteins. *J. Mol. Biol.* **1977**, *115*, 135.
- (29) Richardson, J. S. *Adv. Protein Chem.* **1981**, *34*, 167.
- (30) Wilmot, C. M.; Thornton, J. M. *J. Mol. Biol.* **1988**, *203*, 221.
- (31) Sieber, V.; Jurnak, F.; Moe, G. R. *Proteins: Struct. Funct. Genet.* **1995**, *23*, 32.

MA9900582